International Journal of Applied Pharmaceutics

ISSN- 0975-7058 Vol 14, Issue 5, 2022

Short Communication

COMPARATIVE STUDY OF THE LOADING AMOUNT OF DRUG WITHIN MESOPOROUS SILICA WITH VARIOUS PORE SIZE

DIAH LIA AULIFA[1], ARIF BUDIMAN[2*]

[1]Department of Pharmaceutical Analysis and Medicinal Chemistry, Faculty of Pharmacy, Universitas Padjadjaran, [2]Department of Pharmaceutics and Pharmaceutical Technology, Faculty of Pharmacy, Universitas Padjadjaran
*Email: arifbudimanapt@gmail.com

Received: 30 Jun 2022, Revised and Accepted: 06 Aug 2022

ABSTRACT

Objective: The loading of drugs into mesoporous silica (MS) is an effective strategy to improve the solubility of poorly water-soluble drugs. Previous reports have stated that the surface area and pore volume of MS can affect drug loading and its crystallization in MS. Therefore, this study aims to elucidate the effect of MS pore size on the maximum drug loading and its dissolution profile.

Methods: The ritonavir (RTV) and itraconazole (ITZ) were encapsulated-MS using the solvent evaporation method. The RTV and ITZ loaded-MS were characterized using differential scanning calorimetry (DSC) and PXRD measurement.

Results: The amorphization of RTV loaded-MPS and ITZ loaded-MPS were confirmed as a halo pattern in the powder X-ray diffraction pattern. The melting peak and the glass transition of RTV and ITZ were not discovered in MS with the pore size of 80 Å (weight ratio of 3:7), while in the RTV and ITZ loaded-MS with the pore size of 45 Å, the melting peak and the glass transition were observed. This indicated that the loading amount of RTV and ITZ with larger pore sizes is higher than the lower sizes.

Conclusion: This study demonstrated that the pore size of MS has a significant effect on the loading amount of drugs in MS.

Keywords: Mesoporous silica, Pore size, Drug loading, DSC curve

DOI: https://dx.doi.org/10.22159/ijap.2022v14i5.45698. Journal homepage: https://innovareacademics.in/journals/index.php/ijap

The aqueous solubility of active pharmaceutical ingredients (API) remains the major challenge in the development of oral dosage forms [1-2]. Recently, approximately 90% of new drug candidates are poorly water-soluble, leading to insufficient bioavailability [3-5]. Therefore, the development of a strategy to improve the aqueous solubility of drugs is needed in the formulation of poorly water-soluble drugs [6, 7]. Drug amorphization is an effective strategy to improve the solubility of poorly water-soluble drugs due to a higher Gibbs free energy [8-10]. However, the formulation of the amorphous drug is thermodynamically unstable and recrystallizes easily after dispersing in aqueous or during storage [11, 12].

Drug loading into mesoporous silica (MS) is a promising strategy to stabilize the drug in the amorphous state [13]. MS can also improve the dissolution rate and apparent solubility of the drug compared to their crystalline counterparts [14, 15]. The two mechanisms of drug crystallization inhibition in MS have been proposed include (1) The drug adsorption on the MS surface due to the molecular interaction between the surface of MS of the drug and (2) the nanoconfinement effect of MS, which lead to suppression of crystal growth of drug [2, 16]. Therefore, the surface interaction of drug-MS and pore volume of MS can affect the drug loading and crystallization inhibition in MS [17, 18].

The pore size of MS was also discovered to influence the dissolution profile of drugs. This is because it directly correlated with the loading amount and the release rate of the drug [19]. A large pore size of MS exhibit a relatively faster drug release in dissolution medium [20]. Meanwhile, when a drug within mesoporous silica is dispersed in a dissolution medium, the rapid dissolution of drugs can be achieved as entrapped drugs are easily diffused out of mesopores [19]. This showed that there is a need for the determination of drug loading below the experimental ones to maximize its effect due to the incomplete release within MS.

Several studies reported the drug loading into MS carriers; however, the effect of pore size on the drug loading and its dissolution profile has remained unclear. Therefore, this study aims to elucidate the effect of MS pore size on the maximum drug loading. Ritonavir (RTV) and itraconazole (ITZ) were used as models of poorly water-soluble drugs, with a molecular weight of over 500 g/mol. The solvent evaporation method was adopted to encapsulate the drug into MS, while the amorphous drugs within MS and the maximum drug loading were characterized by modulated differential scanning calorimetry **(**MDSC) and X-ray powder diffraction (XRPD) analysis.

In this study, the RTV (MW = 720.95 g/mol) and ITZ (MW = 705.64 g/mol) used were purchased from FUJIFILM Wako Pure Chemical Corporation (Osaka, Japan), and ChemShuttle (Hayward, USA), respectively. The chemical structures of the drugs are shown in fig. 1. Meanwhile, MS and FSM were kindly gifted from Taiyo Kagaku., Ltd. (Mie, Japan).

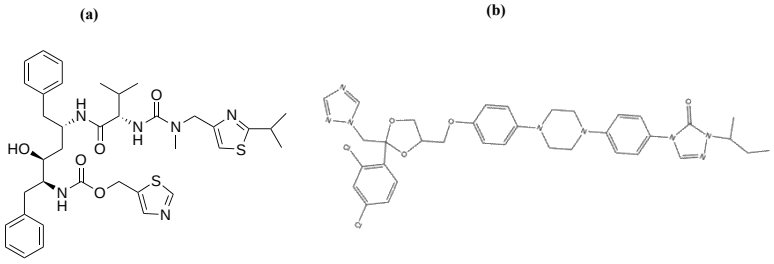

Fig. 1: Chemical structures of (a) RTV, and (b) ITZ

Each drug was dissolved in chloroform and the MPS or FSM was dispersed in the chloroform solution, containing the drug with various weight ratios. The suspension was sonicated at 25 °C for 3 min and evaporated using a rotary evaporator for 30 min at 30 °C. Subsequently, the remaining powder was dried at 30 °C using a vacuum dryer for 48 h to obtain RTV encapsulated into MS (RTV/MS), RTV encapsulated into FSM (RTV/FSM), ITZ encapsulated into MS (RTV/MS), and ITZ encapsulated into FSM (RTV/FSM).

DSC measurement was carried out using a DSC-7000X instrument and approximately 5 mg of the sample was placed into an aluminum DSC pan under an N_2 purge at a flow rate of 40 ml/min. Subsequently, the calorimetric analysis of the samples was measured from 0 to 200 °C.

The PXRD patterns were collected using a Miniflex II with the following conditions, namely 30kV voltage, 15mA current, Cu target, Ni filter, scanning angle of 2θ = 3°-40°, and scanning rate, 4°/min.

In this study, the MS and FSM used were ordered mesoporous silica with a porous texture. Based on the results, the MS and FSM showed a typically irreversible type IV isotherm according to the IUPAC classification, while their pore sizes were 80 Å and 45 Å, respectively.

Ritonavir (RTV) and itraconazole (ITZ) were used as models for poorly water-soluble drugs due to their good glass formers that do not crystallize upon cooling and reheating, which is categorized in class III. Subsequently, the amorphization of each sample was evaluated by PXRD measurement. The RTV crystal exhibited a characteristic diffraction peak in the PXRD patterns, while all ratios of RTV amorphous, RTV/FSM, and RTV/MS showed a hallo pattern without any diffraction peak of RTV crystal in the higher weight ratio (fig. 2). A similar result was also observed in both ITZ/MS and ITZ/FSM (data not shown), which can be due to the low crystallization tendency of RTV and ITZ. Therefore, the amorphization of RTV and ITZ was formed after preparation by the solvent evaporation method. The PXRD result was unable to distinguish whether the drug was inside or outside the pores. This showed that the data cannot determine the loading amount of RTV or ITZ within mesoporous silica.

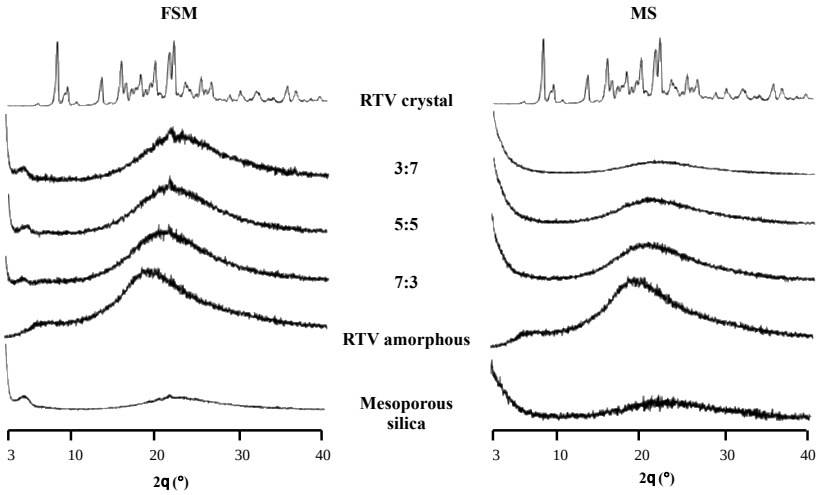

Fig. 2: The PXRD patterns of (a) RTV crystal, RTV amorphous, and RTV/MPS with various weight ratios

The DSC was carried out based on the presence of their melting peaks to evaluate the encapsulation of the drug within the mesoporous silica. Meanwhile, the DSC measurement result of RTV/MS and RTV/is shown in fig. 3. The melting peak of the RTV crystal was observed at 122 °C, while its glass transition temperature (T_g) was observed at 47 °C. However, the melting peak of RTV was not observed in RTV amorphous, RTV/MS, and RTV/FSM due to its good glass formers that do not crystallize upon reheating. Therefore, the presence of T_g was used to determine the encapsulation of RTV within mesoporous silica. The heat capacity changes (ΔCp) of T_g of RTV decreased with a reduction in RTV concentration in MPS, either in RTV/MS system or RTV/FSM system. In RTV/MS, the T_g was not observed in the weight ratio of 3:7. A previous study stated that the absence of T_g was attributed to the successful encapsulation of the drug into MPS [21]. The monomolecular absorption of RTV on the silica surface of MS leads to the absence of T_g in DSC curves. This occurred due to hydrogen bond interaction between the C=O of RTV and the Si-OH of MS. However, the T_g of RTV was still observed in RTV/FSM = 3:7, which indicated that some RTV still existed outside the FSM [22]. Therefore, the amount of RTV encapsulated into MS was higher compared to FSM [23].

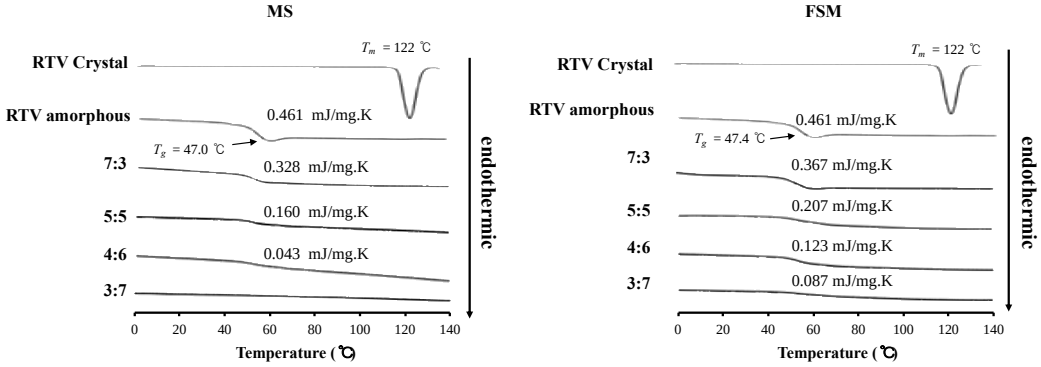

Fig. 3: DSC curve of RTV crystal, RTV amorphous, RTV/MS, and RTV/FSM with various weight ratios

As shown in fig. 4, the concentration of RTV was plotted as a function of Δ*Cp* values of RTV amorphous on the DSC curves to predict the amount of RTV encapsulated into MPS. The fitted lines for RTV/MS and ITZ/FSM systems showed good linearity with correlation coefficients of 0.97 and 0.99, respectively. The loading amount of RTV within MS and FSM, which is represented with y-intercept value, was 30.07 % and 14.83 %, respectively. Therefore, the loading of RTV into MS is more efficient compared to FSM due to its larger pore size.

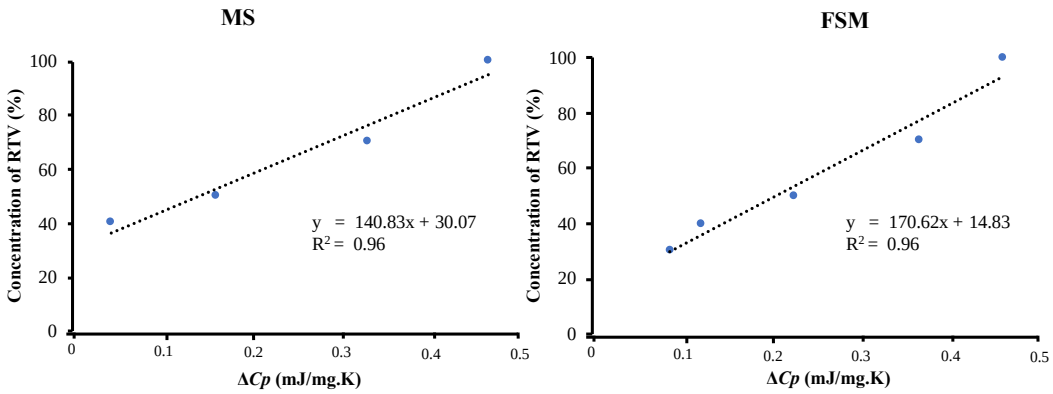

Fig. 4: Plots of RTV concentration against Δ*Cp* of RTV calculated from the DSC curves

Based on the result of DSC measurement from ITZ/MS and ITZ/FSM as shown in fig. 5, the melting peak ITZ crystal was observed at 170.3 °C, while its glass transition temperature (T_g) was observed at 56.7 °C. In the ITZ/FSM system, the heat of fusion decreases with a reduction in ITZ concentration. The melting peak of ITZ crystal was still observed in weight ratios of 3:7, while the melting peak disappeared in ITZ/MS at a ratio of 2:8. Meanwhile, in the ITZ/MS system, the melting peak of ITZ was not observed at a ratio of 3:7. A previous study has reported that the drug within mesoporous silica did not melt in DSC curves because of its amorphous form [24]. The absence of the melting peak of ITZ was attributed to the interaction between the carbonyl and ether groups of ITZ with surface silanol groups through hydrogen bonding, which led to their amorphization after encapsulation into MPS [21]. Therefore, the amount of ITZ encapsulated into FSM was lower compared to MS [23].

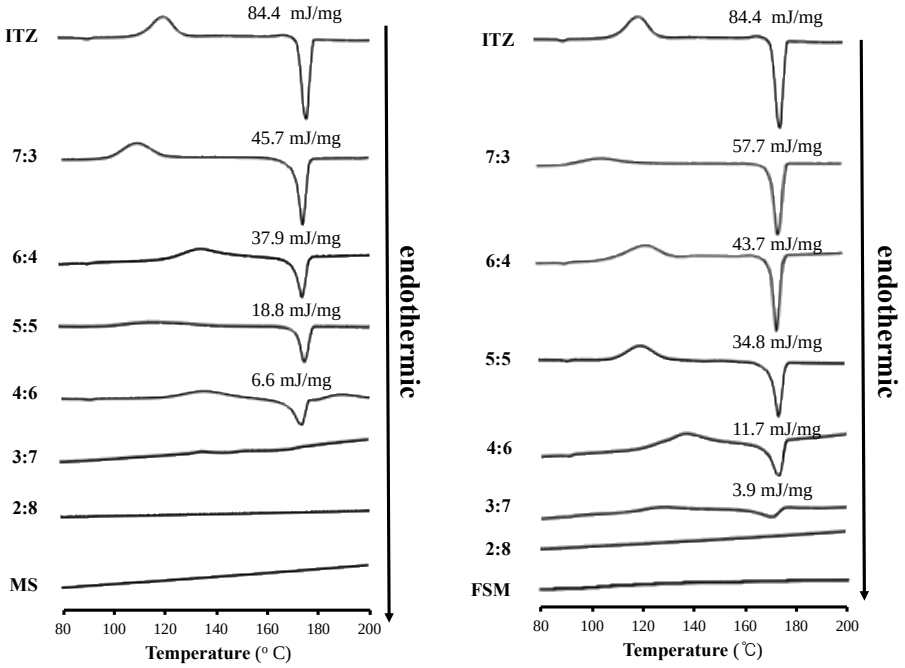

Fig. 5: DSC curve of ITZ amorphous, ITZ/FSM, and ITZ/MS with various weight ratios

The concentration of ITZ was plotted as a function of the heat of fusion on DSC curves as shown in fig. 6 to predict the amount of ITZ encapsulated into MPS. The fitted lines for ITZ/FSM and ITZ/MS systems exhibited good linearity with correlation coefficients of 0.97 and 0.99, respectively. Furthermore, the loading amount of ITZ within FSM and MS, which is represented with y-intercept value, was 25.89 % and 34.27 %, respectively. This showed that the maximum loading amount of ITZ into MS is higher than FSM due to its larger pore size.

Although the amorphization of ITZ was formed in ITZ/MS and ITZ FSM system, the two endothermic peaks of ITZ were observed as shown in fig. 7. These peaks were attributed to the liquid crystal of ITZ with initial temperature values for a smectic to nematic transition at 72.1 °C and a nematic to isotropic transformation at 88.2 °C [25]. The dissolution study was not carried out in the ITZ/MPS system due to the liquid crystal that was being observed.

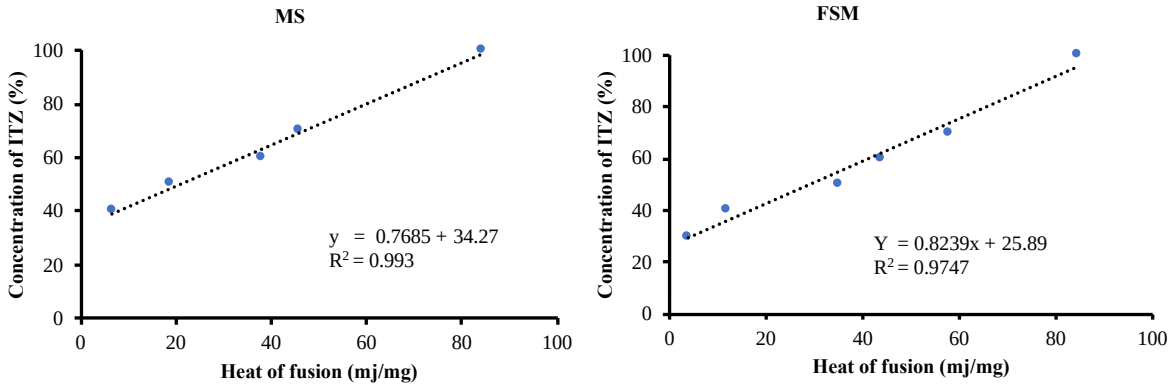

Fig. 6: Plots of ITZ concentration against the heat of fusion of ITZ calculated from the DSC curves

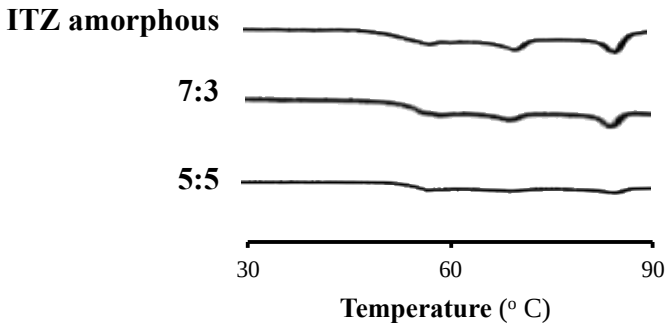

Fig. 7: DSC curve of ITZ amorphous, ITZ/MS = 7:3, and ITZ/MS = 5:5

The effect of pore size on the loading amount of the drug was elucidated. The DSC measurement showed that the loading amount of drug into mesoporous silica with the larger pore size is higher than the lower pore size. This provided fundamental insight into the formulation of drugs encapsulated into MPS, specifically in elucidating the relationship between the pore size of MPS with the loading amount into MPS.

FUNDING

The research was partly supported by a grant from the Ministry of Education, Culture, Research, and Technology of the Republic of Indonesia (KEMENDIKBUDRISTEK, PDUPT) to Arif Budiman (no: 1318/UN6.3.1/PT.00/2022).

AUTHOR CONTRIBUTIONS

All authors have contributed equally.

CONFLICT OF INTERESTS

Declared none

REFERENCES

1. Raghuram M, Alam MS, Prasad M, Khanduri CH. Pharmaceutical cocrystal of prulifloxacin with nicotinamide. Int J Pharm Pharm Sci. 2014;6(10):180-4.
2. Vranikova B, Niederquell A, Sklubalova Z, Kuentz M. Relevance of the theoretical, critical pore radius in mesoporous silica for fast crystallizing drugs. Int J Pharm. 2020 Dec;591:120019. doi: 10.1016/j.ijpharm.2020.120019, PMID 33122108.
3. Adena RSK, Matte KV, Kosuru R. Formulation, optimization, and *in vitro* characterization of dasatinib loaded polymeric nanocarriers to extend the release of the model drug. Int J Appl Pharm. 2021 Sep 7;13(5):318-30.
4. Kawabata Y, Wada K, Nakatani M, Yamada S, Onoue S. Formulation design for poorly water-soluble drugs based on biopharmaceutics classification system: basic approaches and practical applications. Int J Pharm. 2011 Nov 25;420(1):1-10. doi: 10.1016/j.ijpharm.2011.08.032, PMID 21884771.
5. Dening TJ, Taylor LS. Supersaturation potential of ordered mesoporous silica delivery systems. Part 1: Dissolution performance and drug membrane transport rates. Mol Pharm. 2018 Jul 9;15(8):3489-501. doi: 10.1021/acs.molpharmaceut.8b00488, PMID 29985627.
6. Skorupska E, Jeziorna A, Potrzebowski MJ. Thermal solvent-free method of loading of pharmaceutical cocrystals into the pores of silica particles: A case of naproxen/picolinamide cocrystal. J Phys Chem C. 2016 Jun 23;120(24):13169-80. doi: 10.1021/acs.jpcc.6b05302.
7. Skorupska E, Kazmierski S, Potrzebowski MJ. Solid state NMR characterization of ibuprofen: nicotinamide cocrystals and new idea for controlling release of drugs embedded into mesoporous silica particles. Mol Pharm. 2017 May 1;14(5):1800-10. doi: 10.1021/acs.molpharmaceut.7b00092, PMID 28403609.
8. Okada H, Ueda K, Yasuda Y, Higashi K, Inoue M, Ito M. Correlation between drug dissolution and resistance to water-induced phase separation in solid dispersion formulations revealed by solid-state NMR spectroscopy. Int J Pharm. 2020 Mar 15;577:119086. doi: 10.1016/j.ijpharm.2020.119086, PMID 31991185.
9. Murdande SB, Pikal MJ, Shanker RM, Bogner RH. Solubility advantage of amorphous pharmaceuticals: II. Application of quantitative thermodynamic relationships for prediction of solubility enhancement in structurally diverse insoluble pharmaceuticals. Pharm Res. 2010 Dec;27(12):2704-14. doi: 10.1007/s11095-010-0269-5, PMID 20859662.
10. Babu NJ, Nangia A. Solubility advantage of amorphous drugs and pharmaceutical cocrystals. Cryst Growth Des. 2011 Jul 6;11(7):2662-79. doi: 10.1021/cg200492w.
11. Azad M, Moreno J, Dave RR. Stable and fast-dissolving amorphous drug composites preparation via impregnation of Neusilin® UFL2. J Pharm Sci. 2018 Jan 1;107(1):170-82. doi: 10.1016/j.xphs.2017.10.007, PMID 29031953.
12. Yamamoto K, Kojima T, Karashima M, Ikeda Y. Physicochemical evaluation and developability assessment of co-amorphouses of low soluble drugs and comparison to the co-crystals. Chem

Pharm Bull (Tokyo). 2016;64(12):1739-46. doi: 10.1248/cpb.c16-00604, PMID 27733735.
13. Czarnobaj K, Prokopowicz M, Greber K. Use of materials based on polymeric silica as bone-targeted drug delivery systems for metronidazole. Int J Mol Sci. 2019 Mar 15;20(6):1311. doi: 10.3390/ijms20061311, PMID 30875887.
14. Qian S, Heng W, Wei Y, Zhang J, Gao Y. Coamorphous lurasidone hydrochloride–saccharin with charge-assisted hydrogen bonding interaction shows improved physical stability and enhanced dissolution with pH-independent solubility behavior. Crystal Growth & Design. 2015 Dec 3;15(6):2920-8. doi: 10.1021/acs.cgd.5b00349.
15. McCarthy CA, Zemlyanov DY, Crean AM, Taylor LS. Comparison of drug release and adsorption under supersaturating conditions for ordered mesoporous silica with indomethacin or indomethacin methyl ester. Mol Pharm. 2020 Jul 7;17(8):3062-74. doi: 10.1021/acs.molpharmaceut.0c00489, PMID 32633973.
16. Andersson J, Rosenholm J, Areva S, Lindén M. Influences of material characteristics on ibuprofen drug loading and release profiles from ordered micro-and mesoporous silica matrices. Chem Mater. 2004 Oct 19;16(21):4160-7. doi: 10.1021/cm0401490.
17. Antonino RSCMQ, Ruggiero M, Song Z, Nascimento TL, Lima EM, Bohr A. Impact of drug loading in mesoporous silica-amorphous formulations on the physical stability of drugs with high recrystallization tendency. Int J Pharm X. 2019 Dec 1;1:100026. doi: 10.1016/j.ijpx.2019.100026, PMID 31517291.
18. Bavnhøj CG, Knopp MM, Madsen CM, Lobmann K. The role interplay between mesoporous silica pore volume and surface area and their effect on drug loading capacity. Int J Pharm X. 2019 Dec 1;1:100008. doi: 10.1016/j.ijpx.2019.100008, PMID 31517273.
19. Shen SC, Ng WK, Chia L, Hu J, Tan RB. Physical state and dissolution of ibuprofen formulated by co-spray drying with mesoporous silica: effect of pore and particle size. Int J Pharm. 2011 May 30;410(1-2):188-95. doi: 10.1016/j.ijpharm.2011.03.018, PMID 21419202.
20. Thomas MJ, Slipper I, Walunj A, Jain A, Favretto ME, Kallinteri P. Inclusion of poorly soluble drugs in highly ordered mesoporous silica nanoparticles. Int J Pharm. 2010 Mar 15;387(1-2):272-7. doi: 10.1016/j.ijpharm.2009.12.023, PMID 20025947.
21. Budiman A, Aulifa DL. Characterization of drugs with good glass formers in loaded-mesoporous silica and its theoretical value relevance with mesopores surface and pore-filling capacity. Pharmaceuticals (Basel). 2022 Jan 13;15(1):93. doi: 10.3390/ph15010093, PMID 35056149.
22. Budiman A, Higashi K, Ueda K, Moribe K. Effect of drug-coformer interactions on drug dissolution from a coamorphous in mesoporous silica. Int J Pharm. 2021 May 1;600:120492. doi: 10.1016/j.ijpharm.2021.120492, PMID 33744448.
23. Liu N, Higashi K, Kikuchi J, Ando S, Kameta N, Ding W. Molecular-level understanding of the encapsulation and dissolution of poorly water-soluble ibuprofen by functionalized organic nanotubes using solid-state NMR spectroscopy. J Phys Chem B. 2016 May 19;120(19):4496-507. doi: 10.1021/acs.jpcb.6b00939, PMID 27123961.
24. Tanabe S, Higashi K, Umino M, Limwikrant W, Yamamoto K, Moribe K. Yellow coloration phenomena of incorporated indomethacin into folded sheet mesoporous materials. Int J Pharm. 2012 Jun 15;429(1-2):38-45. doi: 10.1016/j.ijpharm.2012.03.011, PMID 22446085.
25. Kozyra A, Mugheirbi NA, Paluch KJ, Garbacz G, Tajber L. Phase diagrams of polymer-dispersed liquid crystal systems of itraconazole/component immiscibility induced by molecular anisotropy. Mol Pharm. 2018 Sep 25;15(11):5192-206. doi: 10.1021/acs.molpharmaceut.8b00724, PMID 30252481.